THE INITIATION, PROPAGATION AND TERMINATION OF ANODE EFFECTS IN HALL-HÉROULT CELLS

TMS[1], Gary Tarcy[2] and Alton Tabereaux[3]
[1]TMS (The Minerals, Metals & Materials Society); 184 Thorn Hill Rd.; Warrendale, PA 15086, USA
2Alcoa Technical Center, 100 Technical Drive, Alcoa Center, PA 15069, USA

Keywords: [1] Alcoa Inc; [2]Consultant

Abstract

Anode effects in Hall-Héroult cells have been the subject of multiple investigations and studies. The current state of the knowledge is fairly well advanced and there is very little discrepancy or controversy with respect to many of the phenomena associated with anode effects. Included in this is the belief they are: 1) AE are the predominate emitter of PFC into the atmosphere 2) AE are triggered by low alumina concentrations near the anode surface 3) Short circuiting of at least part of the anode cathode inter electrode gap is required to terminate an anode effect. This paper will cover some of less discussed aspects of anode effect including: 1) the initiation at a single random anode in the circuit; 2) propagation to multiple anodes until the whole circuit is on anode effect and; 3) reason it is necessary to short circuit the anodes to terminate anode effect.

Introduction

The Initiation and Propagation of Anode Effects

The initiation of anode effect is known to be caused by the depletion of alumina at which point a critical current density is reached and the pot then goes into anode effect. Although not fully confirmed, the most respected correlation for the critical current density has been published by Piontelli (1). Figure 1 depicts how the Piontelli correlation predicts the critical current density to vary for a typical pot. The critical current density becomes smaller (easier for the cell to exceed and thus have an anode effect) for either lower alumina concentrations or cooler temperatures.
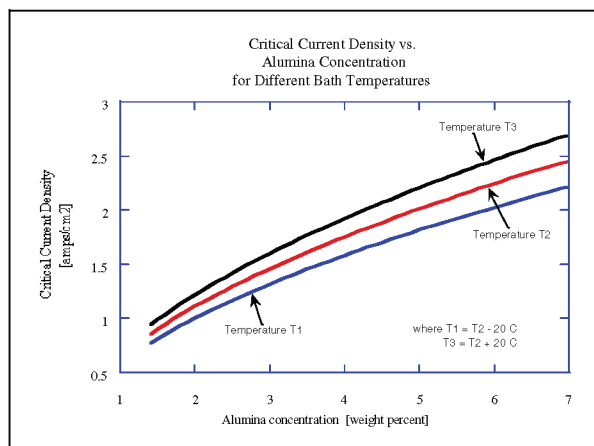

Figure 1. Critical current density vs. alumina concentration for different bath temperatures

Mechanistically this correlation can be explained by:

1) Change in the electrolysis reaction from being a predominately CO_2 producing reaction to more of a CO producing reaction. The CO production result is twice as much gas.
2) Dewetting of the anode as the alumina becomes lower thus having less real anode surface available for electrolysis
3) Different anodes draw different amounts of current and the alumina concentration becomes more non-uniform in concentration in the pot as the pot gets closer to anode effect. Resulting in the anode effect usually being initialized at a single anode and then propagating to the rest of the anodes.
4) The overall voltage on the pot begins to increase due to the increased bubble coverage on the pot and the change in the anode reaction to a more kinetically unfavorable condition.

Figure 2 below shows the changes in CO_2 and CO concentrations measured off of a single anode as the pot approaches anode effect (2). The measurements were made by drilling a hole and inserting a steel pipe completely to the bottom of the anode to assure a minimum contribution from the Boudouard reaction. Infrared was used to measure both the CO and CO_2 concentrations. The significance of this measurement with respect to anode effect initiation is that there is a change in the primary reaction at the anode as the anode effect is approached. The usual reaction:

$$Al_2O_3 + 3/2C \rightarrow 2Al + 3/2CO_2 \qquad (1)$$

which is thermodynamically favored but kinetically hindered due to the difficulty in breaking carbon to carbon bonds get replaced with the thermodynamically favored but usually kinetically hindered reaction

$$Al_2O_3 + 3C \rightarrow 2Al + 3CO \qquad (2)$$

The low alumina concentration in the pot is the cause for the shift in reactions. Although under most circumstances it is more difficult to break the carbon-carbon bonds the increasing lack of oxygen bearing anion leads to the competing reaction becoming more favorable. Finally at anode effect due to even further depletions of alumina approximately 16% of the gas produced from the anode becomes CF_4 and this gas is evolved from the bottom of the anode. The balance of the gas at anode effect is essentially CO and this is produced off the sides of the anode.
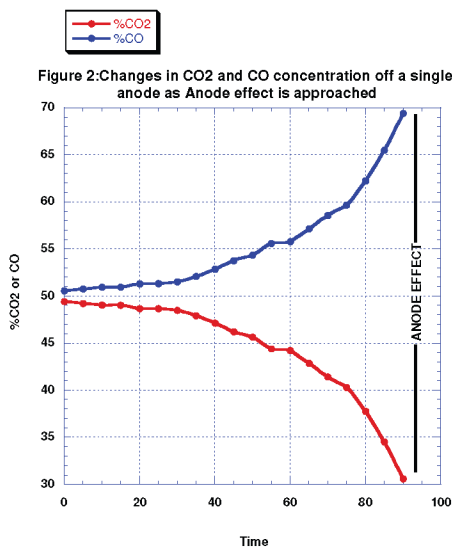
Figure 2: Changes in CO2 and CO concentration off a single anode as Anode effect is approached

Figure 2. Changes in CO_2 and CO concentration off a single anode as a Anode effect is approached.

Figure 3 below shows the onset of anode from an Alcoa P-225 pot. Due to the special design of the pot every anodes current is measured and recorded by the computer every second. The figure shows the usual sequence of events. Prior to the onset of anode effect (in this example it is approximately 3 minutes before) one of the anodes begins to under load with respect to the rest of the group due to the change in reaction cited above. The CO producing reaction in the Hall-Héroult case requires more energy to run and produces more gas thus insulating the anode that is running out of alumina at the fastest rate. This shifts the amperage (in this example 50% of the amperage) that the under loading was carrying to the other anodes in the circuit. The overall low alumina concentration in the pot then leads to more anodes reaching the critical current density In the end the anode effect eventually spreads in a cascading series phenomenon as the current density increases significantly on the remaining anodes until all anodes in the cell are on anode effect.

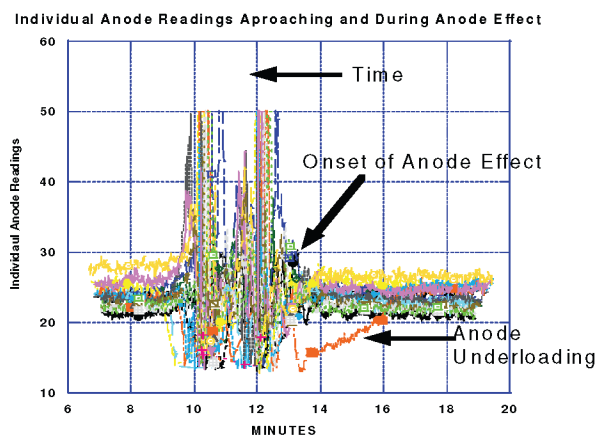Individual Anode Readings Aproaching and During Anode Effect

Figure 3. Individual Anode Current Readings Approaching and During Anode effect

Figure 4 shows the position of the under loading anode where the anode effect was first detected. The study was on 13 pots over a two week period. All positions were responsible for the initiation of the anode effect there is no pattern by which the positions trigger an anode effect. In other words the position effect is essentially random.
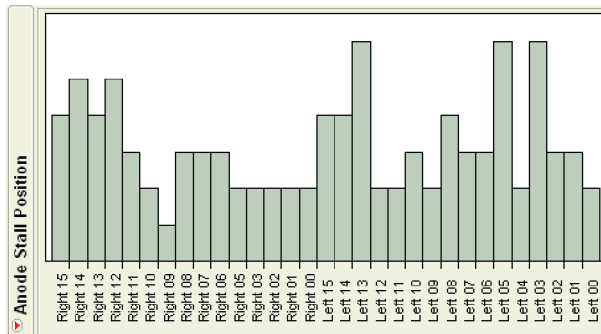
Figure 4. Distribution of the first unloading anode with respect to position in the pot

Figure 5 shows the distribution of the "warning time" from the under loading anode prior to anode effect. The signal detection criteria shows that 95% of the anode effects can be detected in sufficient time (30 seconds prior to anode effect) that action should be able to be taken to prevent anode effects.

Figure 5: Distribution of the Early Warning of Anode effects
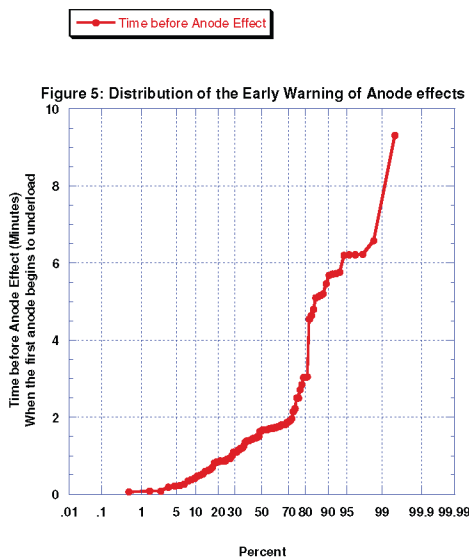
It is clear that anode effect starts at a localized location probably due to a local low alumina concentration under some anodes. This is caused by a combination of a local low superheat, insufficient transport of alumina underneath the anode, or carbon dust blocking the surface of the anode. The location of anodes with the lowest alumina was shown above to vary in the cells in essentially a random manner.

Modeling results by Feng et.al (3) demonstrate that constraining the bath flow underneath anodes by reducing the ACD results in greater extremes of alumina concentration. It was also reported

that there is a stagnant zone in the ACD under the middle of each anode because the alumina in that area is being consumed at a faster rate than it is being replaced during the under-feed period. This seems to indicate that the anode effect initiation may even be more localized than even a single anode and could start in even localized areas of the single anode.

Moxnes et.al. (4) reported that the alumina feed was changed from a "flat, equal feed in the five point feeders to an equal or "flow-adaptive" feed among the five feeders in the SU4 potline at Sunndal, Norway. The alumina distribution in the cells was made more equal by increasing the alumina feed at the two feeders nearest the ends of the cells and decreased the alumina feed in the feeders near the center of the cell. As a result the number of anode adjustment, anode spikes and deformation decreased. It is further anticipated that the more uniform alumina distribution in the cell will result in decreasing the anode effect frequency as well as decreasing sludge residing in the cathode.

Finally, one more interesting observation. There is a small fraction of the time when there is no warning at all that an anode effect is about to occur. If this observation is coupled with the reality that the only actions that can be taken to terminate the anode effect is to lower the anode beams and feed alumina. Lowering the anode beams is the fastest possible countermeasure that could be employed to prevent anodes but this action will take at least several seconds to be effective. Using a 30 second recognition time to react to the anode effect we can calculate the absolute minimum anode effect frequency that we can get if we were 100% successful in preventing every anode effect we observed with the anode under loading technique at least 30 seconds prior to the full anode effect occurring. The calculations are only for the Alcoa P-225 situation and may not extrapolate to all the other technologies but we have calculated the absolute minimum anode effect frequency to be 0.002 anode effects per pot day. This is both encouraging and discouraging. It is encouraging because it points out there remains plenty of room for further improvement, but it is discouraging because it also means that a true zero rate frequency may not be possible with the technology we know of today.

The highly irregular current distribution after the anode effect is due the after effect oscillations in the metal pad surface.

Terminating Anode Effects

To sucessfully terminate (or kill) anode effects in operating cells requires a short circuit to the molten aluminum metal. Once the short-circuit occurs in cells the anode effect is killed instantly.

- Anode effects are killed by first adding alumina to the bath of cells and then manually inserting a wood pole under anodes into the metal, resulting in a large expulsion of combustion gases that causes molten aluminum to splash upward and short-circuit with anodes. This manual process usually requires minutes, and even longer in some circumstances

- Anode effects are typically killed in prebake cells using automatic anode effect termination programs in the computer system by: 1) rapidly adding a sufficient amount of alumina in order to increase the alumina content in the bulk bath all around the cell and, 2) the

anode beam (with all anodes) are moved down to decrease the anode to cathode distance (ACD) to cause electrical short-circuits between anodes and aluminum waves. Anodes effects can often be killed quickly <5 seconds using this practice.

In addition to the rapid feed of alumina to bath by point feeders during the anode effect, the increase in anode immersion and the intense bath circulation produced by the metal wave causes the liquid bath to come into contact with the anode cover which is a source of alumina all around the pot. Another source of alumina is by some sludge dissolution that is removed by the metal waves from the cathode surface [9]. The intense bath circulation due to metal waves and high bath temperature (>1000 °C) quickly increases the bulk alumina concentration in the cell bath and importantly makes it more homogeneous throughout the cell.

The isolating layer of PFC gas is removed by the combination of short-circuits on anodes, and the decrease in anode current density due to the deeper anode immersion when the ACD is reduced on all anodes.

Conventional methods of extinguishing anode effects by electrical shorting were not effective in a drained TiB2-G cathode cell as it did not have an aluminum metal pool (5). All attempts to extinguish anode effects by electrical shorting the pilot cell failed The only effective method of extinguishing anode effects during drained operation involved the momentary interruption of power to the cell.

Impact of Short-Circuiting During AE Termination on PFC Emissions

Lower PFC Emissions From Soderberg Cells

Marks (6) reported revised Tier 2 PFC slope coefficients that demonstrate that the emission rates for PFC gases is substantially less for Soderberg cells, (0.092) compared with prebake cells (0.143-0.272) during anode effects.

When the pot is on anode effect a high fraction of the electrical current is conducted from the sides of the anode, because the isolating gas layer considerably hinders the flow of current though the bottom surface. This produces an important increase in the horizontal current densities and therefore of the MHD instabilities of the pot during the anode effects. The anode effect is inherently unstable in Soderberg cells as the bath immersion on the sides is only about one tenth of that for prebake cells. The pot develops a wave in the bath-metal interface that provides local short-circuits to the Soderberg anode. Tabereaux et.al. and Marks et.al. (7) reported that intermittent short-circuiting observed in Soderberg cells is linked to a decrease in PFC emissions.

The emission rate of CF_4 gas from the Soderberg cell shown in Figure 6 is ~46% less than prebake cells that have continuous emission with minimal short-circuits. The lower rate of PFC emissions due to electrical shorting agrees with the lower values determined for the Tier 2 PFC Slope factors for Soderberg cells (0.092) compared with center-break and side-break prebake cells (0.14 to 0.27)
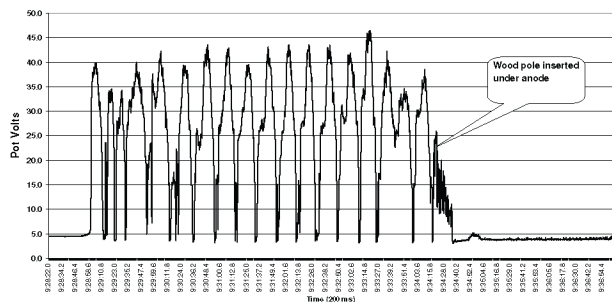
Figure 6. Electrical Shorting During Anode Effect of VS Soderberg Cell

Differences in PFC Emission Rates in Prebake Cells

The major difference in PFC emission coefficients (determined by the "slope" and "anode overvoltage" methods) between individual prebake smelters especially those using the same technology, is largely due to differences in the anode effect kill strategy. The emission of PFC gases stop, or are greatly reduced each time anodes are short-circuited with metal. Thus the manner and timing in which the anodes are lowered to cause short-circuit with the metal pad waves in order to kill the anode effects has a great influence on the rate of PFC generation in prebake cells (8).
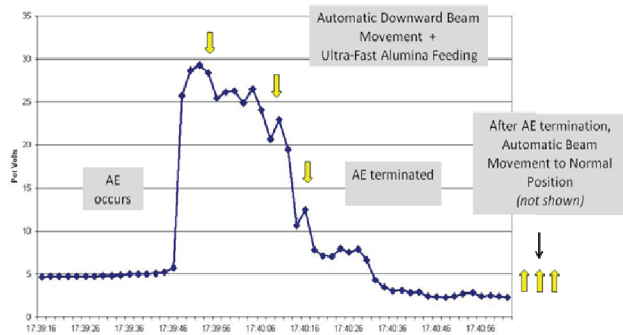

Figure 7. Anode effect Killed in Prebake Cell by Electrical Shorting with Fast, Aggressive Down Moves.

1. Slow AE kill with anode pumping by slow multiple cycles of reducing and increasing the ACD until strong short-circuit with metal waves: Slow pumping of anodes results in a non-linear decreasing emission of PFC gases during the anode effect.

2. Faster AE kill with modified anode pumping utilizing faster, deeper ACD down moves until strong short-circuit with metal waves: Faster pumping of anodes results in a less irregular emission of PFC gases during the anode effect.

3. Fast AE kill with large, aggressive ACD down moves causing fast, strong short-circuit with metal waves as shown in Figure 7: Deep fast down move of anodes results in one small linear peak emission of PFC gases during the anode effect.

4. Fast AE kill with a smaller ACD down move until MHD instability occurs and a self-sustained wave develops that causes instant short-circuits on anodes and intense bath

circulation: Fast down move of anode typically results in one small emission peak of PFC gases during the anode effect (9).

Conclusion:

Anode effects are initiated by the local depletion of alumina at a single anode resulting in a shift in the primary gas producing reaction. This shift leads to production of twice the amount of gas for the same amount of current which leads to a decrease in the amount of current carried by this anode. The load is shifted from this anode to other anodes and the trend continues until the whole cell comes to anode effect. The anode effect must then be terminated by s short circuit resulting in breaking of the PFC insulating film. The usual method of short circuiting also results in partial immersion of the anode cover into the liquid bath along with increased stirring of the bath from the high degree of instability. This raise the alumina concentration overall and diminishes any localalize alumina depleted regions of the cell.

References

1. Piontelli, R., Mazza, B. and Pedeferri, P. (1965). Ricerche sui fenomeni anodici nelle celle per alluminio. Metallurgia Italiana, 57(2), 51-69.

2. Internal Alcoa Letter A. J. Sharkins to Rolf Rolles 1979-12-26.

3. Y. Feng, M.A. Cooksey, and M.P. Schwarz, "CFD Modelling of alumina Mixing in Aluminum Reduction Cells", Light Metals 2010, pp.455-460.

4. B. Moxnes, A. Solheim, M. Liane, E. Svinsas and A. Halkjelsvik, « Improved Cell Operation by Redistribution of the Alumina Feeding", Light Metals 2009, pp.461-466.

5. G.L. Fredrickson,"1999 Pilot Cell Operations – Final Report", (DOE Project # DE-FC07-97ID13567), March 2000.

6. Marks, J., "Method for Calculating the PFC Emissions From Primary Aluminum Production," Light Metals 2006, pages 185-188.

7. Marks, J., Tabereaux, A.T., Pape, D., Bakshi and E. Dolin, "Factor affecting PFC Emissions From Commercial Aluminum Reduction Cells", Light Metals 2001, pp.295-302.

8. A. Tabereaux, "Maximum Anode Effect Voltage", Light Metals 207, pages pp.405-410.

9. P. Navarro, Gregoric G., Cobob O., and Calandra, A., "A New Anode Effect Quenching Procedures", Light Metals 2003, pp.479-486.